BEILSTEIN JOURNAL OF NANOTECHNOLOGY

Supporting Information

for

Synthesis of biowaste-derived carbon-dot-mediated silver nanoparticles and the evaluation of electrochemical properties for supercapacitor electrodes

Navya Kumari Tenkayala, Chandan Kumar Maity, Md Moniruzzaman and Subramani Devaraju

Beilstein J. Nanotechnol. **2025,** *16,* 933–943. doi:10.3762/bjnano.16.71

Experimental procedures including materials details and characterizations; Schematic representation; BET isotherm and pore size distribution plot; SEM, EDX, and elemental mapping of PG-CDs-AgNPs; ASC device fabrication method; Table for the comparison of cyclic stability

S1. Experimental section

Materials

All the chemicals were used without further purification. Silver nitrate ($AgNO_3$) was purchased from Sisco Research Laboratories, India. Dimethyl sulfoxide (DMSO, 99.5%), potassium chloride (KCl), tetraethylammonium tetrafluoroborate ($TEABF_4$, 99%), and ethanol were purchased from Sigma-Aldrich, India. Deionized (DI) water was used for all syntheses and experiments.

Preparation of *Pongamia pinnata* leaves powder

Waste *Pongamia pinnata* leaves were collected from nearby places, washed with distilled water, and dried in the hot air woven at 70 °C. Then, using a mortar and pestle, the dried leaves were ground into fine powder and used for further processing.

Material characterization

Using a Shimadzu UV 1800 spectrophotometer, the UV–visible absorption spectra of PG-CDs and PG-CDs-AgNPs were acquired. The PL emission spectra of PG-CDs and PG-CDs-AgNPs were taken using a spectrophotometer (RF 6000, Shimadzu, Japan). X-ray diffraction patterns of PG-CDs-AgNPs were measured using a powder X-ray diffractometer (Model-D8 Advance Bruker AXS powder XRD). At a degassing temperature of 60 °C for 4 h, BET analysis and pore size distribution of the samples were measured via N_2 adsorption–desorption method using the Micromeritics' ASAP 200. A Thermo Fisher Scientific-MultiLab-2000, (monochromated Al Kα source) was used for the XPS analysis. A Hitachi's scanning electron microscope (SEM) (SU8600) was utilized to visualize the surface morphologies (operating

voltage: 5kV) and elemental mapping of Ag, C, and O. By using a JEOL JEM-ARM200F (operating voltage: 200kV), transmission electron microscopy (TEM) analysis was performed.

Electrochemical characterization

For three-electrode analysis, cyclic voltammetry (CV), galvanostatic charging/discharging (GCD), and electrochemical impedance spectroscopy (EIS) were performed using 1 M aqueous (aq.) KCl as the electrolyte on a Biologic SP200 electrochemical workstation. Pt foil and Ag/AgCl were utilized as the counter and reference electrodes in the three-electrode configuration, while the electroactive materials (PG-CDs-AgNPs) [sample: carbon black: binder (Nafion) = 80:15: 5] were mounted on the flat surface of a graphite rod to fabricate the working electrode. For GCD and CV analyses in the aqueous electrolyte, a potential limit of 0.0–0.8 V was maintained to prevent the overpotential of H_2O. The EIS study was carried out between 1 MHz and 1 Hz at room temperature. The gravimetric specific capacitance (SC) of PG-CDs-AgNPs was calculated applying the following equation [1]:

$$SC\ (F/g) = \frac{i \times t}{m \times \Delta V} \qquad (S1)$$

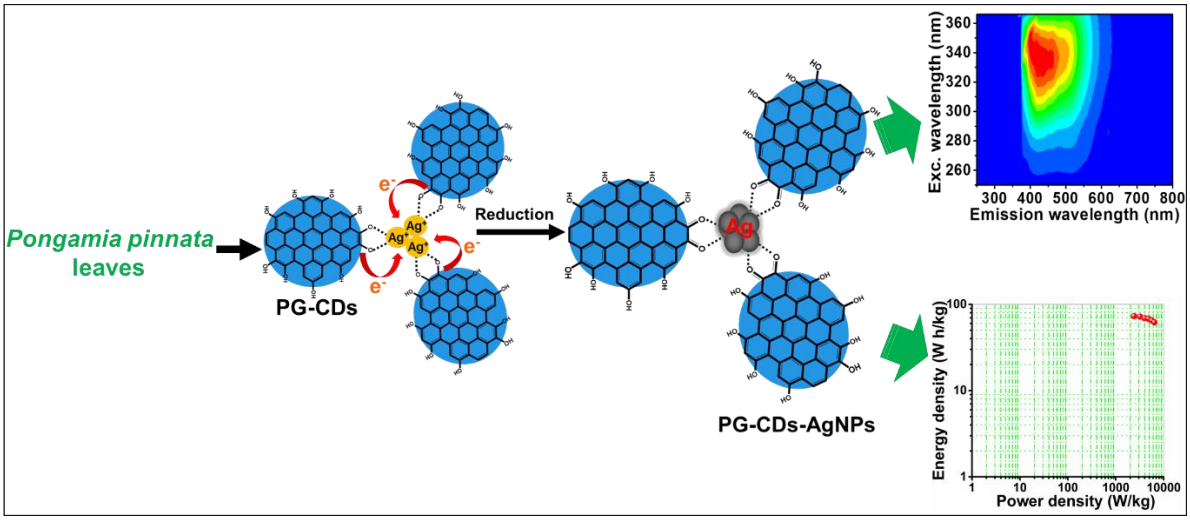

Scheme S1: Schematic representation of the overall methodology as well as the optical and electrochemical storage properties of PG-CDs-AgNPs.

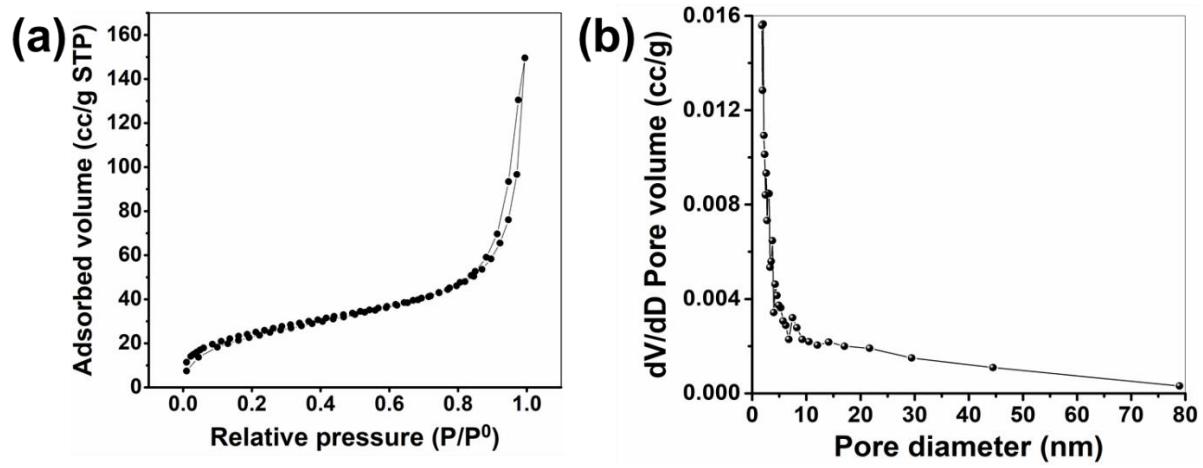

Figure S1: (a) BET isotherm and (b) pore size distribution plot of PG-CDs-AgNPs.

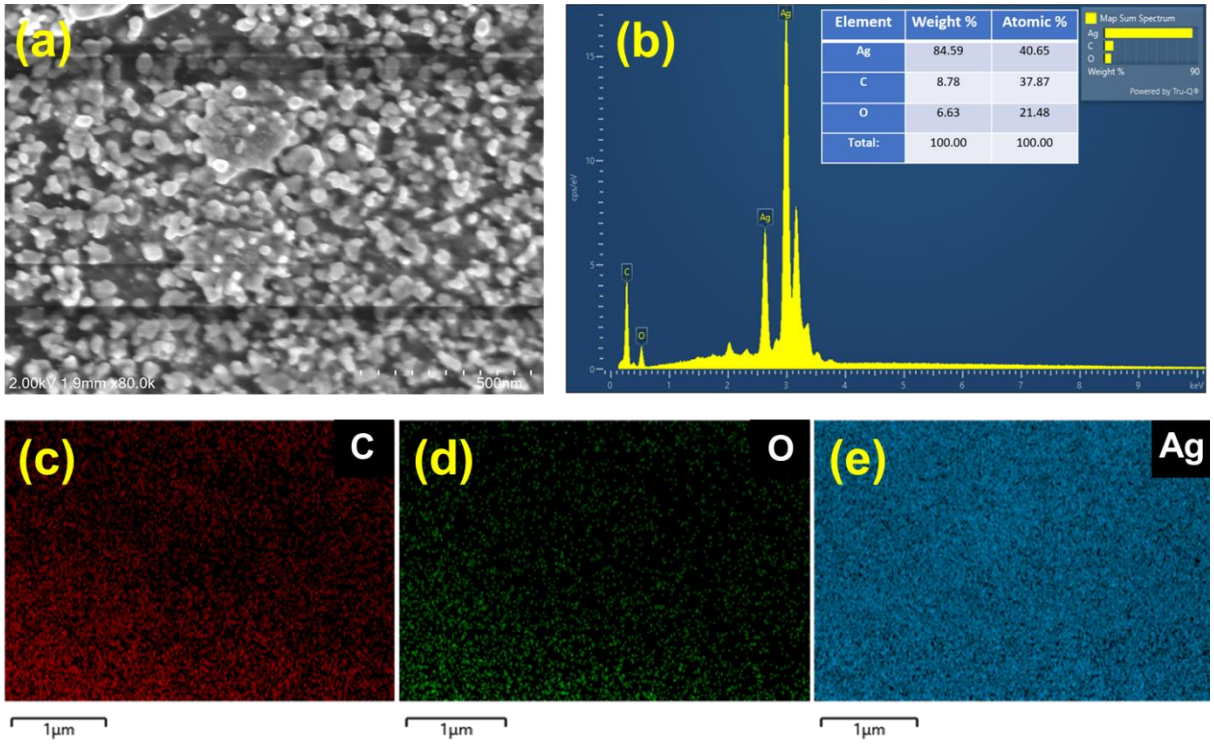

Figure S2: (a) SEM image of PG-CD-AgNPs, (b) EDX analysis of PG-CD-AgNPs, and (c–e) Elemental mapping of C, O, and Ag, respectively for PG-CD-AgNPs.

S2. Asymmetric supercapacitor device fabrication method

For the fabrication of an asymmetric supercapacitor (ASC) device, PG-CD-AgNPs and carbon black (CB) were used as positive and negative electrodes, respectively; whereas tissue paper acted as the separator. In a manner similar to [2], the ASC device was fabricated. The electrochemical analyses of the supercapacitor device were conducted using an organic electrolyte [1M tetraethylammonium tetrafluoroborate ($TEABF_4$)/ dimethyl sulfoxide (DMSO)] on a Biologic SP200 electrochemical workstation.

The gravimetric specific capacitance (SC) of the device was calculated applying the following equation [1]:

$$SC\ (F/g) = \frac{2 \times i \times \Delta t}{m \times \Delta V} \qquad (S2)$$

The specific energy density (ED) and power density (PD) of the ASC device were calculated using the following equation [1]:

$$ED\ (W\ h/kg) = \frac{SC \times \Delta V^2}{7.2} \qquad (S3)$$

$$PD\ (W/kg) = \frac{ED \times 3600}{\Delta t} \qquad (S4)$$

Table S1: Comparison of the cyclic stability of the PG-CDs-AgNPs nanohybrid (as the positive electrode used in ASC) with other similar electrodes.

Electrode	Measurement type	Cyclic stability	Reference
Sn/SnO_2/GQD/CNF	As positive electrode in ASC	86.1% After 5000 cycles	[3]
Graphene oxide/CDs/ Polypyrrole	Symmetric supercapacitor	92.9% After 5000 cycles	[4]
AgNPs/Porous carbon	As positive electrode in ASC	82.7% After 10000 cycles	[5]
NF/NiSe/MnO_2-LCDs	As positive electrode in ASC	88.46% After 7000 cycles	[6]
Ag QDs/$NiMoO_4$	As positive electrode in ASC	84.4% After 5000 cycles	[7]
Ag quantum dots/MoO_3	As positive electrode in ASC	90% After 5000 cycles	[8]
Pt-AgNPs/rGO	Symmetric supercapacitor	70.65% After 10000 cycles	[9]
Ag@Ti_3C_2	As anode in ASC	91.27% After 5000 cycles	[10]
Zn–MoS_2/CDs@BN	As positive electrode in ASC	89% After 10000 cycles	[11]
NiCo-LDH@CDs	As positive electrode in ASC	78.6% After 10000 cycles	[12]
CDs/Ni-Zn phosphates	As positive electrode in ASC	90.6% After 10000 cycles	[13]
PG-CDs-AgNPs	As positive electrode in ASC	87% After 10000 cycles	This work

GQD: graphene quantum dot, CNF: carbon nanofiber, NF: nickel foam, LCDs: lignin-derived carbon dots, rGO: reduced graphene oxide, BN: boron nitride, and LDH: layered double hydroxide.

References

1. Chuai, M.; Zhang, K.; Chen, X.; Tong, Y.; Zhang, H.; Zhang, M. *Chem. Eng. J.* **2020,** *381,* 122682. doi:10.1016/j.cej.2019.122682.
2. Maity, C. K.; De, S.; Acharya, S.; Siddiki, S. H.; Sahoo, S.; Verma, K.; Thakur, V. K.; Nayak, G. C. *J. Energy Storage* **2022,** *56,* 105928. doi:10.1016/j.est.2022.105928.
3. Li, Z.; Zhang, C.; Bu, J.; Zhang, L.; Cheng, L.; Wu, M. *Carbon* **2022,** *194,* 197–206. doi:10.1016/j.carbon.2022.03.079.
4. Zhang, X.; Wang, J.; Liu, J.; Wu, J.; Chen, H.; Bi, H. *Carbon* **2017,** *115,* 134–146. doi:10.1016/j.carbon.2017.01.005.
5. Wang, R.; Li, X.; Nie, Z.; Jing, Q.; Zhao, Y.; Song, H.; Wang, H. *J. Energy Storage,* **2022,** *51,* 104364. doi:10.1016/j.est.2022.104364.
6. Xie, X.; Xu, Y.; Liu, J.; Wang, D. Lv, T.; Yuan, F.; Zhang, Q. *ACS Appl. Mater. Interfaces* **2024,** *16,* 68157-68168. doi:10.1021/acsami.4c13282.
7. Zhang, X.; Li, Z.; Yu, Z.; Wei, L.; Guo, X. *Appl. Surf. Sci.* **2020,** *505,* 144513. doi:10.1016/j.apsusc.2019.144513.
8. Zhang, X.; Fu, Q.; Huang, H.; Wei, L.; Guo, X. *Small,* **2019,** *15,* 1805235. doi:10.1002/smll.201805235.
9. Punnakkal, N.; Chandhana, J. P.; Nair, D.; Thomas, S. S.; Madhavan, A.; TG, S. B.; Vasu, S. P. *J. Power Sources* **2025,** *641,* 236819. doi:10.1016/j.jpowsour.2025.236819.
10. Alam, A.; Saeed, G.; Kim, K. W.; Kim, J. K.; Park, H. S.; Lim, S. *J. Energy Storage* **2023,** *72,* 108227. doi:10.1016/j.est.2023.108227.
11. Maity, C. K.; De, S.; Panigrahi, A.; Acharya, S.; Verma, K.; Kim, M. J.; Nayak, G. C. *Compos. B: Eng.* **2023,** *264,* 110887. doi:10.1016/j.compositesb.2023.110887.
12. Wang, S.; Deng, J.; Li, M.; Lin, J.; Luo, L.; Yuan, Z.; Zhang, W.; He, C.; Du, G.; Zhao, W. *Chem. Eng. J.* **2025,** *511,* 162275. doi:10.1016/j.compositesb.2023.110887.
13. Guo, M.; Wang, S.; Zhao, L.; Guo, Z. *Electrochim. Acta* **2018,** *292,* 299-308. doi:10.1016/j.electacta.2018.08.119.